RASĀYAN *J. Chem.*
Vol. 16 | No. 2 |728-734| April - June | 2023
ISSN: 0974-1496 | e-ISSN: 0976-0083 | CODEN: RJCABP
http://www.rasayanjournal.com
http://www.rasayanjournal.co.in

SYNTHESIS OF $LiFe_{1-x}Ni_xPO_4/C$ USING THE REFLUX WITH MICROWAVE IRRADIATION METHOD

D. Purwaningsih✉, H. Sutrisno, K. H. Sugiyarto, C. Kusumawardani and N. A. Kusumaningrum

Department of Chemistry Education, Faculty of Mathematics and Natural Sciences, Universitas Negeri Yogyakarta-YO 55281 Indonesia

✉Corresponding Author: dyah_purwaningsih@uny.ac.id

ABSTRACT

The aim of this study was to synthesize $LiFe_{1-x}Ni_xPO_4/C$ with x = 0; 0.05; 0.07; 0.09 using the reflux method assisted by microwave irradiation. The goal was to increase the value of the electronic conductivity and reaction rate of Li^+ compounds. The results showed that the method successfully synthesized $LiFePO_4/C$ and $LiFe_{1-x}Ni_xPO_4/C$ with an orthorhombic crystal structure in the *Pnma* space group. The optimum reflux-microwave irradiation time was 10 minutes, and increasing moles of Ni doping lead to a decrease in the lattice parameters cell volume. The crystalline size ranged from 21.42–22.62 nm, and the surface of the compound particles was irregular. The compound $LiFe_{0.93}Ni_{0.07}PO_4/C$ had the highest conductivity (5.45×10^{-7} S/cm).

Keywords: $LiFePO_4$, $LiFe_{1-x}Ni_xPO_4/C$, Microwave, Orthorhombic, *Pnma*

RASĀYAN *J. Chem.*, Vol. 16, No. 2, 2023

INTRODUCTION

The use of $LiFePO_4$ as a material for lithium-ion batteries shows promise due to its long-lasting nature, good cycle stability, environmental friendliness, and relatively low cost. However, the rigid orthorhombic olivine structure of $LiFePO_4$ leads to low electronic conductivity and Li^+ reaction rate, preventing the battery from reaching its full theoretical capacity.[1] Therefore, it is necessary to modify the compound to increase its electronic conductivity and Li^+ reaction rate. Various technical methods have been used to overcome these issues, including coating the particles with carbon-based materials[2], doping $LiFePO_4$ with super-valent cations[3], and reducing the particles to the nanoscale.[4] While these methods have been carried out separately, combining only two of them could lead to better results.[5] Doping $LiFePO_4$ with metal elements can increase the lattice deficiency, which has the potential to improve the lithium-ion diffusion rate and the internal conductivity of the particles. This is especially important for addressing the poor conductivity and electrochemical performance of $LiFePO_4$. It is important to focus on different doping positions, as the doping element may vary. Ni^{2+} is a suitable cathode dopant for $LiFePO_4$ batteries due to its similarity to Fe, as both elements are in the same row of the periodic table with similar radii that allow for easy replacement. In addition, Ni doping has been shown to effectively enhance the electrochemical properties of $LiFePO_4$.[6] In this study, the reflux method assisted by microwave irradiation was utilized to support the principles of green chemistry. Green chemistry aims to minimize or eliminate the use and/or production of harmful substances during the development, production, and application of chemical products related to a specific synthesis or process.[7] The use of reflux-microwave has the potential for green chemistry since the microwave heating system allows for fast and direct transfer of energy to any absorbent material. This direct transfer of energy to molecules leads to a reduction in reaction time by 10–1000 times and increases the yields and product selectivity. The use of microwave acceleration may be a more environmentally friendly alternative to the conventional method.[8] The present study aimed to synthesize $LiFePO_4$ by incorporating Ni doping and carbon coating using citric acid as the source of carbon. Four different concentrations of Ni dopant, namely 0; 0.05; 0.07; and 0.09 were added to determine their impact on the $LiFe_{1-x}Ni_xPO_4/C$ compound. The synthesized compounds were characterized using XRD, SEM-EDX, and LCR-meter to analyze their crystal structure, lattice parameters, crystallite size, surface morphology, and compound conductivity.

http://doi.org/10.31788/RJC.2023.1628164

EXPERIMENTAL

Precursor Preparation

A 0.3 M solution of LiOH and Fe_2O_3 0.3 M was prepared by dissolving x grams of p.a. Merck LiOH/Fe_2O_3 p.a. Merck in a beaker glass containing 10 mL of distilled water. The mixture was stirred until homogenous and then diluted using ethylene glycol to the solution limit. Similarly, a 0.3 M solution of H_3PO_4 0.3 M was prepared by dissolving x grams of H_3PO_4 in a beaker glass containing 10 mL of distilled water. The solution was stirred until homogeneous and then diluted using ethylene glycol to the solution limit.

Synthesis of $FePO_4$/C

A total of 50 mL of 0.3 M Fe_2O_3 solution, 0.3 M H_3PO_4 solution, 0.1 M citric acid solution in ethylene glycol solvent were added to a reflux flask. The synthesis was carried out at medium temperature (380 Watt) for varying durations of 10, 15, and 20 minutes using a microwave. The resulting compound was then cooled and filtered, and the deposited material was dried in an oven at 150°C for 2 hours. Finally, the dried compound was calcined at 750°C for 3 hours.

Synthesis of $LiFe_{1-x}Ni_xPO_4$/C

A total of 50 mL of a solution containing 0.3 M {(1-x) mol} Fe_2O_3, 0.3 M H_3PO_4 , 0.1 M citric acid, and 0.3 M (x mol) Ni $(CH_3COO)_2$ in ethylene glycol was placed in a reflux flask. The synthesis was carried out using a microwave at medium temperature (380 Watt) for 10 minutes, with time variations. The resulting solution was then cooled and filtered, and the resulting deposit was dried in an oven at 150°C for 2 hours. The dried compound was subsequently calcined at 750°C for 2 hours. LiOH was added by grinding the substance with acetone, and the compound was calcined then again for 3 hours.

Characterization of $LiFe_{1-x}Ni_xPO_4$/C

$FePO_4$/C and $LiFe_{1-x}Ni_xPO_4$/C compounds were characterized using X-Ray Diffraction (XRD) with a Rigaku Miniflex 600-Benchtop instrument that utilized CuKα radiation (λ = 1.5406) at room temperature, covering a range of 2θ between 10°–80°. Two types of software were used to process the XRD data: Match for qualitative analysis and Rietica for quantitative analysis. Surface morphology and composition were examined by SEM-EDX analysis. Electrical conductivity was measured using an LCR-meter (EUCOL U2826) with a frequency of 20Hz–5MHz and at a voltage level of 1 volt. The samples were converted into pellets on silver plating and the LCR-meter data was then analyzed using Zview software.

RESULTS AND DISCUSSION

Optimizing Synthesis Time

The synthesized compounds were then tested using XRD, and the results of the test are presented in Fig.-1 in the following. The diffractogram shows that synthesized compounds had peaked in several time variations. The $FePO_4$/C compound was optimally synthesized during 10 minutes of radiation, as demonstrated by the compounds containing the least impurities, shown in Fig.-1. The impurities or other phases in the compound were identified as Fe_2O_3 and $Fe_2O_7P_2$ based on COD 96-101-1241.

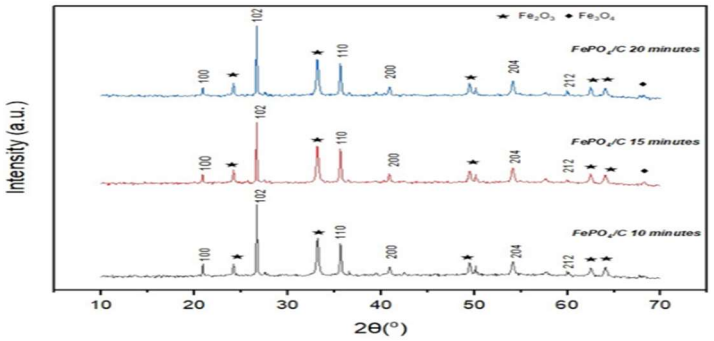

Fig.-1: Diffractogram of $FePO_4$/C

The result of the quantitative analysis, performed using Rietica software, is presented in Table-1. The compound was tested for its crystal structure, and found to be trigonal with P3121 space group. Based on the data presented in Table-1, the lattice parameter value changed in each time variation. After ten minutes

of radiation, values a and b increased to 5.138412 (Å). For 15 minutes of irradiation, the increase was 5.140017 (Å). Finally, for 20 minutes of radiation, the increase was 5.151225 (Å). The value of c decreased after 10 minutes of radiation to 10.864978 (Å), 10.85370 (Å) after 25 minutes, and 10.860272 (Å) after 20 minutes. The volume of $FePO_4$/C increased along with the increase of values a and b.

Table-1: The Result of Rietica Analysis of $FePO_4$/C

Compound $FePO_4$/C	Lattice Parameter			V (Å^3)	Rp	Rwp	GoF(χ^2)
	a (Å)	*b* (Å)	*c* (Å)				
10 minutes	5.138412	5.138412	10.864978	248.437546	3.72	7.55	0.8947
15 minutes	5.140017	5.140017	10.860272	248.485168	3.62	7.01	0.7922
20 minutes	5.151225	5.151225	10.822696	246.807800	3.62	7.45	0.8683

The peaks that show $FePO_4$/C are those with hkl fields of 100, 102, 110, 200, 204, and 212. This indicates that the optimized compound is $FePO_4$/C, although there are some peaks that do not show hkl peaks of the $FePO_4$/C, namely hkl 003, 111, 114, 300, and 303. Therefore, based on the results of qualitative and quantitative data analysis, $FePO_4$/C compound can be optimally obtained during the 10 minutes of microwave irradiation.

The Synthesis of $LiFe_{1-x}Ni_xPO_4$/C

Figure-2 shows the diffractograms of $LiFe_{1-x}Ni_xPO_4$/C (x= 0; 0.05; 0.07; 0.09), indicating that the synthesized compound is the $LiFePO_4$, based on COD number 96-400-1846. The peaks are sharp and reveal the presence of $Li_3Fe_2(PO_4)_3$ as an impurity phase in all compounds.

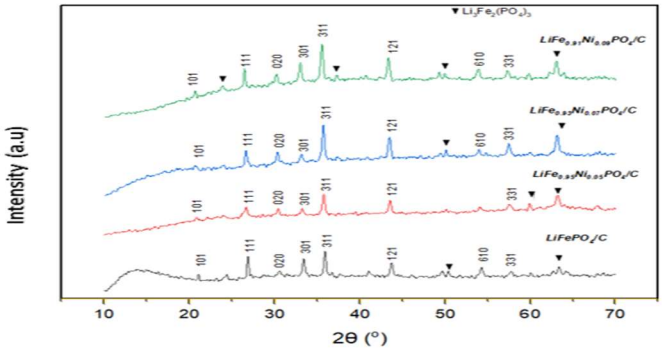

Fig.-2: Diffractograms of $LiFe_{1-x}Ni_xPO_4$/C (x= 0; 0.05; 0.07; 0.09)

The impurities $Li_3Fe_2(PO_4)_3$ are caused by two main types of lithium ferric phosphate (LFP), namely $Li_3Fe_2(PO_4)_3$ or often called NASICON, $Li_2FeTi(PO_4)_3$ or $LiFeP_2O_7$ and $LiFePO_4$ with olivine structure.[9] The content of carbon (C) in $LiFePO_4$ compound coating was not detectable, likely due to the low concentration added or its amorphous state.[10] The diffraction peak for Ni doping was not detected, but the diffractogram shows that Ni doping had an influence, as shown in hkl area 311. In this area, there was Ni mol doping that was added in $LiFePO_4$/C. The doping causes a shift in the peak of the 311 hkl area, which increases with the number of Ni doping moles. At x values 0; 0.05; 0.07; and 0.09, the shift in the hkl 311 field is 2θ 35.83°; 35.69°; 35.78°; and 35.58° respectively. The effect of Ni doping on the XRD peak of the 311 hkl area is evident, as the increase in doping concentration causes the peak position to shift towards a larger angle.[10] This effect on the diffractogram is not limited to the 2θ value shift of the 311 hkl plane. In Fig.-2, it can be observed that the XRD also experienced an increase in intensity with the increase in doping concentration, except for the sample x = 0.05, which had a lower intensity value. Specifically, the intensity value in sample x = 0.05 is 845 lower than the intensity value in sample x = 0, which was 976. The shift in XRD peak after nickel doping was primarily caused by iron, a multivalent element that is easily oxidized during the synthesis process to produce $LiFePO_4$ products, resulting in a lower crystalline peak. Nickel substitution can eliminate iron oxidation, favoring the formation of a product with a higher peak intensity than undoped $LiFePO_4$.[11] Table-2 presents the result of the Rietica analysis, including the lattice parameters and the volume of the compounds, indicating an orthorhombic crystal structure with a Pnma space group. The lattice parameters show that a ≠ b ≠ c. The difference in Ni doping concentration causes changes in the lattice

parameters and volume of the compounds. The lattice parameter b decreases in value due to the replacement of Fe^{2+} ions (0.78 Å) by Ni^{2+} ions (0.69 Å). Yang *et al.* (2015) explain that the addition of Ni doping caused the [FeO_6] site, originally formed by the Fe-O bond, to be replaced by [NiO_6] formed by the Ni-O bond, both of the same order. The decrease in lattice parameter values after carbon coating and Ni doping indicated that Ni enters the $LiFePO_4$ lattice without affecting the phospho-olivine structure.[12] In addition to the lattice parameters, the effect of the volume due to Ni concentration can be seen in Fig.-3.

Table-2: The Result of Rietica Analysis of $LiFe_{1-x}Ni_xPO_4/C$ (x= 0; 0.05; 0.07; 0.09)

	Lattice Parameter			V (Å ^{3})	Rp	Rwp	GoF(χ^2)
	a (Å)	*b* (Å)	*c* (Å)				
$LiFePO_4/C$	10.271272	6.269180	4.637563	298.624	4.48	6.41	1.72
$LiFe_{0.95}Ni_{0.05}PO_4/C$	10.204585	6.218843	4.624595	293.480	5.31	6.62	1.196
$LiFe_{0.93}Ni_{0.07}PO_4/C$	10.31598	5.989327	4.738294	288.311	4.00	5.66	1.65
$LiFe_{0.91}Ni_{0.09}PO_4/C$	10.365344	5.881534	4.678133	285.198	4.49	6.33	2.44

Figure-3 illustrates the effect of Ni concentration on the volume, which decreases as the moles of Ni doping increased, except for when 0.05 moles of doping were used, which caused an increase in volume from 285 Å^3 to 298 Å^3 . The increase could be attributed to the small amount of Ni, which entered $LiFePO_4$. The cell volume decreased as more Ni was added, owing to the larger radius of the Fe^{2+} compared to that of the Ni^{2+} ion. The decrease was directly proportional to the decrease in lattice parameters, as any change in the lattice parameter also resulted in a change in, the volume. The decrease in volume and lattice parameters induced by Ni doping and carbon coating was expected to enhance the electrochemical performance of the cathode.

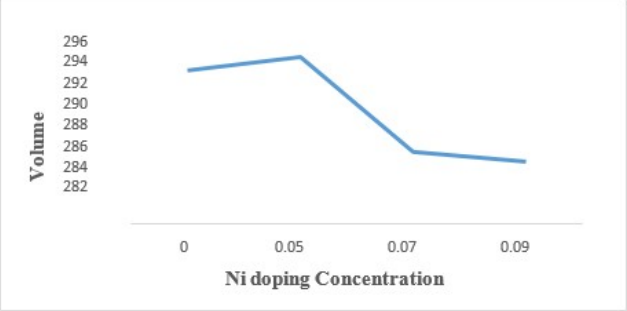

Fig.-3: Graph of Ni-doping Mole Relationship and Volume

Crystallite Size Analysis

The crystallite size data are presented in Table-3. Ni doping resulted in a reduction in the crystallite size of the compound. The smallest crystallite size was observed for x = 0.07. A smaller crystallite size in a particle shortened the diffusion path of the Li^+ ion and increased the electrochemical activation area, which enhanced the electrochemical properties of the cathode material.[6] Figure-4 shows the relationship between moles of Ni doping and crystallite.

Table-3: Crystallite Size

X	Crystallite Size (nm)
0	22.62
0.05	21.54
0.07	21.42
0.09	21.70

Morphological Analysis and Compound Composition

The SEM test image in Fig.-5 shows an irregularly shaped compound with an indistinct surface. The particle size of the compound appears to be varied, and the particles seem to agglomerate and combine with each other. The EDX data provide information on the atomic mass composition of the compound, revealing the presence of Fe (48.62%), P (0.38%), O (36.63%), and C (6.7%), resulting in the mole ratio of Fe: P: O of 1:0.014 :0.448. Besides these atoms, Fig.-6 shows the existence of Al and Si impurities.

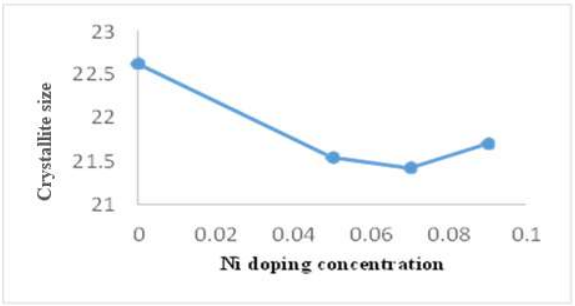

Fig.-4: Graph of Ni-doping Mole and Crystallite Size Relationship

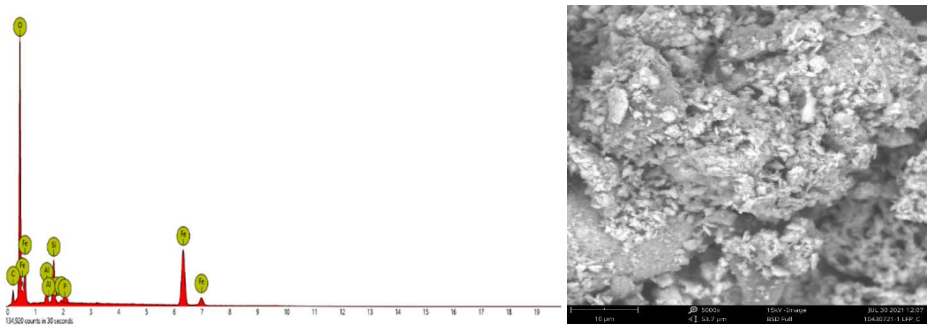

Fig.-5: The SEM-EDX Image of $LiFePO_4/C$ at 10000x Magnification

The SEM-EDX image of $LiFe_{0.93}Ni_{0.07}PO_4/C$, presented in Fig.-6, shows smaller grains than the $LiFePO_4/C$ compound. This smaller particle size indicates the success of Ni doping in $LiFePO_4/C$. Additionally, in Fig.-6, fine grains can be observed attached to the larger particles. The EDX analysis indicates the presence of Fe, P, O, C, and Ni atoms with a mole ratio of 262.5: 0.54: 1: 71.33, which is not in accordance with the theoretically expected mole ratio of Fe: Ni: P: O, which should be 0.93: 0.07: 1:4. The observed discrepancy is not surprising and could be due to the appearance of other phases in the compound, which might have altered the mole ratio of the compound. Furthermore, it is important to note that EDX analysis is not the most accurate for determining elemental content.

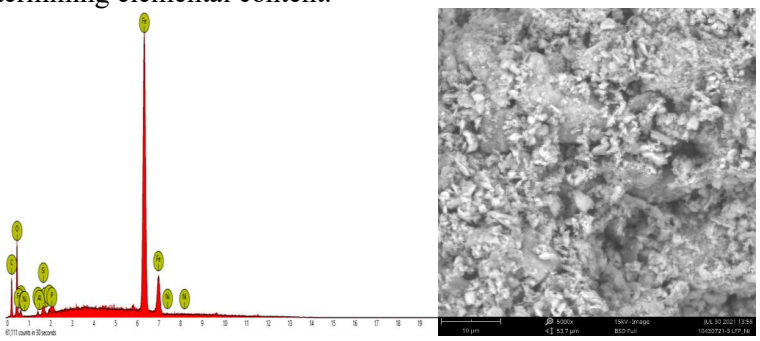

Fig.-6: SEM Image and its-EDX of $LiFe_{0.93}Ni_{0.07}PO_4/C$

Electrical Conductivity Analysis

The electrical conductivity analysis was carried out to evaluate the impact of Ni doping on the conductivity of the $LiFePO_4/C$. The compound was prepared using the reflux-microwave irradiation method, and its conductivity was tested using an LCR meter. The results were then analyzed using the Electrochemical Impedance Spectroscopy (EIS) method. The findings indicated that there was an increase in the conductivity of the compound after Ni doping. The increase in conductivity could be attributed to the ion exchange mechanism present in the $LiFePO_4/C$ samples. Electrical conductivity testing was performed to evaluate the charge-discharge performance of the battery in terms of capacity and electrical conductivity. A higher electrical conductivity implies better battery charge-discharge performance.[13] Figure-7 shows the results of the conductivity testing of the four samples in the Cole-Cole plot. The semicircle curve formed in the plot is related to the value of charge transfer resistance and 56-electron resistance. The different arc diameters for the four samples can also be seen in Fig.-7. The $LiFe_{0.95}Ni_{0.05}PO_4/C$ sample had the largest

diameter, while the $LiFe_{0.93}Ni_{0.07}PO_4/C$ sample had the smallest. This semicircle diameter indicates the resistive properties of a material. The larger the arc diameter the lower the ionic conductivity. The decrease in conductivity is caused by the large current resistance which slows down the electrons. A high charge transfer resistance value leads to lower conductivity.

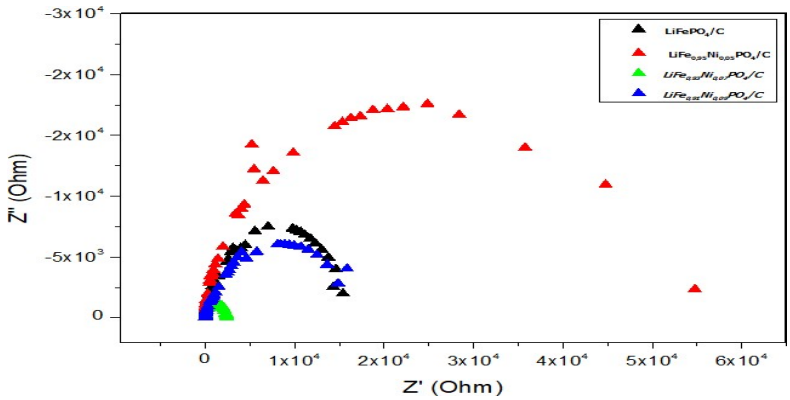

Fig.-7: Cole-Cole Curve of the Sample

The results of the EIS analysis are presented in Table-4. It can be observed that the sample with the highest conductivity value is $LiFe_{0.93}Ni_{0.07}PO_4/C$, with a conductivity value of 5.45×10^{-7} S/cm. On the other hand, the $LiFePO_4/C$ sample exhibited the lowest conductivity value of 7.78×10^{-8} S/cm. These results indicate the successful doping of Ni metal to increase the material's conductivity. Furthermore, Table-4 also reveals that the sample conductivity was superior to the theoretical conductivity of 10^{-9} S/cm. This improvement in conductivity was attributed to the addition of carbon in the $LiFePO_4$ compound. When the carbon was evenly distributed on the surface, it generated an electric field due to its electrostatic nature, which caused a Coulomb or electrostatic force on the presence of Li ions. This force accelerates the movement of the lithium-ion charge on the evenly distributed carbon layer, making it easier for lithium ions to move.[14]

Table-4: Sample Conductivity Data

Sample	Conductivity (S/cm)
$LiFePO_4/C$	7.78×10^{-8}
$LiFe_{0.95}Ni_{0.05}PO_4/C$	2.62×10^{-8}
$LiFe_{0.93}Ni_{0.07}PO_4/C$	5.45×10^{-7}
$LiFe_{0.91}Ni_{0.09}PO_4/C$	7.42×10^{-8}

Variations in the mole of Ni doping in the $LiFe_{1-x}Ni_xPO_4/C$ sample showed the highest conductivity value of 5.45×10^{-7} S/cm at 0.07 Ni doping, which can be attributed to the phases formed in the sample. XRD data analysis of the three doping variation samples revealed that the $LiFe_{0.93}Ni_{0.07}PO_4/C$ sample had the least impurity or impurity phase, resulting in a higher load of the $LiFePO_4$ phase compared to the other doping variation samples. The higher the load of the $LiFePO_4$ phase in the sample, the higher the conductivity value.

CONCLUSION

The compound $LiFe_{1-x}Ni_xPO_4/C$ was successfully synthesized using the reflux-microwave irradiation method. The data analysis concluded that $LiFePO_4/C$ and $LiFe_{1-x}Ni_xPO_4/C$ were compounds with an orthorhombic crystal structure and *Pnma* space group. However, the synthesized compounds were not pure but contained other phases. The lattice parameters of the compounds changed after doping, with values ranging from a = 10.204585 – 10.365344 Å; b = 5.881534 – 6.269180 Å; c = 4.624595 – 4.738294 Å, and a volume ranging from 285.198 – 298.624 Å.[3] The crystal size of the doped compound decreased to a range of 21.42–22.62 nm. The surface morphology of the compounds $LiFePO_4/C$ and $LiFe_{0.93}Ni_{0.07}PO_4/C$ was irregular. The conductivity value of the compound increased after doping, with the best conductivity value observed in the $LiFe_{0.93}Ni_{0.07}PO_4/C$ compound, which was 5.45×10^{-7} S/cm. In short, the study showed that Ni metal doping could increase the conductivity of $LiFePO_4/C$ compounds.

ACKNOWLEDGMENTS

The support provided by Universitas Negeri Yogyakarta through the 2021 Research Grant Project was instrumental for this work, and the authors are grateful for it. The authors also thank Hari Muryanto for editing the final draft prior to publication.

CONFLICT OF INTERESTS

The authors declare that there is no conflict of interest.

AUTHOR CONTRIBUTIONS

All the authors contributed significantly to this manuscript, participated in reviewing/editing and approved the final draft for publication. The research profile of the authors can be verified from their ORCID ids, given below:

D. Purwaningsih https://orcid.org/0000-0003-2546-0954
H. Sutrisno https://orcid.org/0000-0002-0461-9041
K. H. Sugiyarto https://orcid.org/0000-0002-9963-4331
C. Kusumawardani https://orcid.org/0000-0002-3001-6236
N. A. Kusumaningrum https://orcid.org/0009-0000-3910-2280

REFERENCES

1. W. U. Ling, Z. X. Wang, X. H. Li, L. J. Li, H. J. Guo, J. C. Zheng, and X. J. Wang, *Transactions of Nonferrous Metals Society of China*, **20**, 5 (2010), https://doi.org/10.1016/S1003-6326(09)60219-3
2. T. V. S. L. Satyavani, A. S. Srinivas Kumar, and P. S. V. Subba Rao,*Engineering Science and Technology, an International Journal,* **19**, 1 (2016), https://doi.org/10.1016/j.jestch.2015.06.002
3. Y. Yang, K. Li, and H. Li, *International Journal of Applied Ceramic Technology*, **12**, 1(2015), https://doi.org/10.1111/ijac.12139
4. T. H. La, N. T. Nguyen, T. M. A. Nguyen, In *Proceedings of the 5th Asian MaterialsData Symposium, Hanoi – Vietnam,* pp.343–352(2016), https://doi.org/10.1021/jp8053058
5. H. C. Shin, S. B. Park, H. Jang, K.Y. Chung, W. I. Cho, C. S. Kim, and B. W. Cho *Electrochimica Acta*, **53**, 27 (2008), https://doi.org/10.1016/j.electacta.2008.06.005
6. H. Yuan, X. Wang, Q. Wu, H. Shu, and X. Yang, *Journal of Alloys and Compounds*, **675**, 187(2016), https://doi.org/10.1016/j.jallcom.2016.03.065
7. F. A. Bassyouni, S. M. Abu-Bakr, and M. A. Rehim, *Research on Chemical Intermediates*, **38**, 2, (2012), https://doi.org/10.1007/s11164-011-0348-1
8. J. Zhao and W. Yan, *Modern Inorganic Synthetic Chemistry*, 173-175(2011), https://doi.org/10.1016/B978-0-444-53599-3.10008-3
9. Y. Liu, Y. J. Gu, G. Y.Luo, Z. L. Chen, F.Z. wu, X.Y. Dai, Y. Mai, and J.Q. Li, *Ceramics International,* **46**, 10 (2020), https://doi.org/10.1016/j.ceramint.2020.03.011
10. P. S. Suci, M. Zainuri, and E. Endarko, *Materials Science Forum,* **964**, 45(2019), https://doi.org/10.4028/www.scientific.net/MSF.964.45
11. H. X.Tung, D. P. Luan, and N. N. Tru, *Journal of Science and Technology*, **55**, 1B(2017), https://doi.org/10.15625/2525-2518/55/1B/12119
12. Y. Ge, X. Yan, J. Liu, X. Zhang, J. Wang, X. He, R. Wang, H. Xie, *Electrochimica Acta*, **55**, 20(2010), https://doi.org/10.1016/j.electacta.2010.05.040
13. C. Gong, Z. Xue, S. Wen, Y. Ye, and X. Xie, *Journal of Power Sources*, **318**, 93(2016), https://doi.org/10.1016/j.jpowsour.2016.04.008
14. M. Zainuri, B. A. Subagyo, and E. Novialent, *Materials Science Forum*, **966**, 456(2019), https://doi.org/10.4028/www.scientific.net/MSF.966.456

[RJC- 8164/2022]